THE EFFECT OF INFECTION ROUTE ON DISEASE OUTCOME IN RATS INFECTED WITH RIFT VALLEY FEVER VIRUS

by

Aaron Wyland Walters

B.S. Neuroscience, Westminster College, 2012

Submitted to the Graduate Faculty of

the Department of Infectious Diseases and Microbiology

Graduate School of Public Health in partial fulfillment

of the requirements for the degree of

Master of Science

University of Pittsburgh

2016

UNIVERSITY OF PITTSBURGH

Graduate School of Public Health

This thesis was presented

by

Aaron Walters

It was defended on

12/07/2016

and approved by

Douglas S. Reed, Ph.D.
Associate Professor
Department of Immunology
School of Medicine
University of Pittsburgh

Joshua T. Mattila, Ph.D.
Assistant Professor
Department of Infectious Diseases and Microbiology
Graduate School of Public Health
University of Pittsburgh

Thesis Advisor: Amy L. Hartman, Ph.D.
Assistant Professor
Department of Infectious Diseases and Microbiology
Graduate School of Public Health
University of Pittsburgh

Amy Hartman, PhD

THE EFFECT OF INFECTION ROUTE ON DISEASE OUTCOME IN RATS INFECTED WITH RIFT VALLEY FEVER VIRUS

Aaron Walters, M.S.

University of Pittsburgh, 2016

ABSTRACT

Rift Valley fever virus (RVFV) is a mosquito-borne pathogen which has the potential of causing severe outbreaks in both livestock and humans. These outbreaks are currently confined mostly in Africa and the Arabian Peninsula, but have the potential to spread to many locations. Symptomatic humans can experience a wide range of disease features, but most infected people develop a self-limited febrile illness (fever and body aches). In 1-2% of cases, more severe forms develop, including encephalitis or hemorrhagic fever. The case fatality rate of the encephalitic and hemorrhagic form of the disease is 50%. Because no licensed vaccine exists to prevent this viral infection, further research on the pathogenesis of the virus must be completed to further our understanding.

The most poorly understood form of RVF is the encephalitic form. Our lab uses a rat model of lethal encephalitis involving aerosol infection with RVFV. This study has 2 aims: 1) To better understand disease caused in rats after different routes of infection. Our lab's research on RVFV has to date focused primarily on the aerosol infection route, so this study implemented alternate routes of infection to map the outcome of disease progression. 2) To measure the vascular integrity of the brain in aerosol infected rats to determine if breakdown of the blood brain barrier occurs.

Our results from Aim 1 demonstrated that intranasal and aerosol infections caused the highest lethality. Intragastric and intratracheal routes did not consistently establish lethal infection in the animals. Confirming prior results, the subcutaneous route of infection established the lowest mortality in Lewis rats, with nearly all rats surviving infection after receiving a high dose. For Aim 2, we found that the blood brain barrier breaks down after viral penetration into the brain between 4-6 days post infection. This breakdown was especially evident in the olfactory bulb, cerebellum, and cortex of infected animals. The public health significance of this project is directly related to the exploration of the neuropathogenesis of Rift Valley fever virus, which is currently unknown. Understanding how RVFV establishes infection in host species is the first critical step in vaccine or therapeutic development.

TABLE OF CONTENTS

LIST OF TABLES

LIST OF FIGURES

PREFACE

Without my advisor, Dr. Amy Hartman, no part of this project would have been possible. It was only with her continuous support and direction that I was able to complete this research, which I am forever grateful for. I would also like to thank Dr. Douglas Reed and Dr. Joshua Mattila for their contributions to my research. Dr. Reed was a critical part of my work as he performed all aerosol infections required for my research. Both of their input helped to shape the direction that my research was going. Also, special thanks goes to all the members of the Hartman Lab. Having this quality group of scientists to collaborate with was truly a blessing. A special thanks goes out to my lab mate Michael “The Rainman” Kushowers (Michael Kujawa) for battling through thesis work with me from the very beginning of our journey through the Master of Science program together. I would also like to thank my wife Rebecca for having to put up with me through all of the craziness that is graduate school. She kept my mind focused but still reminded me to have fun and enjoy our journey together. Also, I could never succeed in accomplishing something so substantial in my life without my parents. I know that I will only ever receive love and encouragement from both of them. They have always supported me in everything I have done, and without them I would be lost. I am truly blessed to have so many people in my life that stand with me in all that I do. Thank you all!

1.0 INTRODUCTION

Rift Valley Fever Virus (RVFV) is categorized as a Phlebovirus and belongs to the *Bunyaviridae* family. It was first isolated near the Rift Valley in Kenya in the 1930's and has since spread to many other regions throughout Africa (4). The virus is transmitted via arthropod vectors and has demonstrated the ability to infect both animals and humans throughout Africa and the Arabian Peninsula (1). In the past, RVFV was shown to possess the ability to be transmitted by at least 30 different species of mosquitoes, which significantly increases the potential of the virus to spread globally (1).

Outbreaks of Rift Valley Fever (RVF), which have occurred regularly between 1970 and the present day, have been directly associated with the occurrence of the warm period of El Niño (1). During this natural environmental period, flooding is reported in many regions throughout Africa and the Arabian Peninsula, which ultimately causes excessive mosquito larvae hatches and leads to increased transmission of the virus to both humans and livestock in the affected areas (1). Throughout periods of RVF outbreaks, animals are mainly affected (specifically ruminants), but humans have been shown to be susceptible to infection during these periods as well (3). The economic impact of these outbreaks can be quite devastating due to the abortion storms that occur in pregnant ruminants, and because of the fatalities that can also occur in young or weak ruminants infected by the virus (2).

Generally 2 main types of mosquito genera transmit RVFV: *Culex* and *Aedes* (4). During outbreaks, mosquito transmission of RVFV generally impacts ruminant populations most severely causing an almost 100% neonatal fatality rate and around a 20% mortality rate in other animals (5). Human infections are frequent but fatalities are much less common, with only around 2% of cases progressing to severe complications such as neurological or hemorrhagic disease (5). When cases do progress from flu-like symptoms to more severe forms of the disease, fatality rates in humans can reach as high as 50% (4). Humans are less likely to acquire RVFV infection from mosquito bites; the more likely routes of infection for humans include contacting bodily fluids (blood) from infected animals, and consuming raw milk (4)

The severe forms of RVFV are quite alarming, and considering the number of mosquito species that can propagate the virus to both livestock and humans, there is serious potential for high morbidity and mortality. With recent migrations of mosquitoes and the spread of RVFV to countries further north such as Egypt and Saudi Arabia, this virus could have significant public health and economic impacts with ease of trans-territorial migration (1). There is currently no vaccine or effective therapeutic for human administration, which has contributed to the current classification of RVFV being a potential bioterrorism agent (6). It has long been known that aerosolization is the most likely route of infection for a bioterrorism event including RVFV due to the high mortality rate caused by aerosolization of small viral particulates (6). Understanding viral pathogenesis during different routes of infection, such as aerosolization and mosquito transmission, is essential for the development of a successful vaccine or therapeutic that could prevent or limit the progression of RVFV from reaching the hemorrhagic or encephalitic forms.

1.1 RIFT VALLEY FEVER VIRUS

1.1.1 Virology

Rift Valley fever virus consists of a linear tri-segmented negative sense genome (7). The virus is made up of a small (S) segment, a medium (M) segment, and a large (L) segment (7). The S segment is responsible for encoding a nucleocapsid protein (N) and a nonstructural protein (NSs) (7). The nonstructural protein acts as the major virulence factor and is responsible for circumventing the immune response of the host organism while the nucleocapsid protein functions to prevent degradation of viral RNA (7).

The M segment of the virus codes for a glycoprotein precursor protein (GPC), which is then cleaved into 2 separate structural proteins named Gn and Gc, both of which are essential for virus-cell membrane attachment (7). The M segment also codes for a nonstructural protein and a 78-kDa protein (7). The nonstructural protein functions to resist apoptosis, and the function of the 78-kDa protein still has yet to be defined (7). The L segment is responsible for production of the RNA-dependent RNA polymerase, which functions to generate new viral particles by propelling the original virus through transcription and translation of its viral genome (7). The cellular surface molecule recognized by RVFV for viral attachment and entry into the host cell is largely unknown (7).

1.1.2 Epidemiology

RVFV was first isolated near the Rift Valley in Kenya in 1930 (4). Since then, many outbreaks have been reported throughout Africa, but they have mainly been confined to the sub-

Saharan countries within Africa (4). RVFV follows a life cycle that closely parallels that of all *phleboviridae (4).* The enzootic cycle that maintains the virus involves mainly *Aedes* mosquitoes that can transmit the virus to their offspring via vertical transmission (4). It is in the offspring where the virus can survive during the dry seasons in the highly resilient eggs deposited by adult *Aedes* mosquitoes (4) Epizootic/epidemic outbreaks are linked with rainy seasons or periods of unusual warmth that trigger excessive egg hatches and allow for viral circulation and transmission to secondary vectors including *Culex* mosquitoes (4). Transmission of the virus to secondary vectors only increases the probability of viral infection and establishment in areas previously unblemished by RVFV (4).

RVF is a unique virus not only because it has emerged in new territories, but also because it has demonstrated the capacity to reestablish itself after remaining dormant for many years (8). The first outbreaks were confined mainly to the sub-Saharan countries, but in 1973 and 1987 the first outbreaks were recorded in Sudan and West Africa respectively (8). These outbreaks demonstrated the ability of the virus to shift trans-regionally while still causing generation of successful infection. The first major epidemic occurred during the spread of the virus to Egypt in 1977 (8). Up to 200,000 clinical cases were reported and at least 600 deaths were reported during the Egyptian outbreak (8). Not only did the virus begin an upward migratory shift north towards the Arabian Peninsula, but it also spread to Madagascar from continental Africa in 1991 (8).

Research from the most recent outbreaks of RVF (Kenya, East Africa, Sudan, and Tanzania from 2006-2008) has demonstrated that the epidemiology of the virus is changing (8). Data acquired from historical outbreaks indicated that the virus was most closely associated with livestock infection (8). Recent data from current outbreaks suggests that more human cases are

emerging than in previous RVFV outbreaks, and the mortality rate of those infected is significantly higher than in previously documented outbreaks (6). An outbreak from 2010 in South Africa involved over 237 cases with at least 26 cases that resulted in death, which supports that an epidemiological change in the lethality of the virus is occurring (6).

1.1.3 Pathogenesis and Treatment/Prevention

Humans are mainly infected with RVFV after coming into contact with blood from infected tissues usually from butchering, animal birthing, or from veterinary treatment due to health problems (9). Human exposure to RVFV can result in mild or severe infection (9). The incubation period in human infection can range anywhere from two to six days (9). Mild infection after the incubation period can be identified if the individual experiences a sudden onset of flu-like symptoms, vomiting, sensitivity to light, and joint pain (9). These symptoms can last anywhere from four to seven days or until stimulation of the humoral immune response and antibody-mediated immunity occurs (9). In roughly two percent of cases, RVFV progresses to the severe form of the disease, which can be represented by up to three distinct symptoms: ocular disease, meningoencephalitis, and hemorrhagic fever (9). The ocular form of RVFV can be identified by the formation of lesions in the eyes that develop anywhere from one to three weeks post infection, which usually result in blurry or decreased vision (9). The meningoencephalitic form normally develops one to four weeks after the initial onset of symptoms (9). Distinct features of this form of RVFV infection include loss of memory, hallucinations, convulsions, coma, and in severe cases permanent neurological loss of function (9). The hemorrhagic form of RVFV infection generally develops two to four days after the onset of initial symptoms (9). Apparent signs of this form of the infection include bloody vomit or stool, purple skin rashes

resulting from internal bleeding, and bleeding from the nose or gums (9). If death occurs in the subject, it generally happens anywhere from three to six days after the initial onset of clinical symptoms (9).

The onset of disease in livestock or other animals is very dramatic and occurs shortly after infection with an incubation period of only 12-96 hours in lambs (2). The most intense symptoms occur in younger animals and generally lead to death after only hours of infection (2). Some of the symptoms that occur in infected animals include high temperature, rapid breathing, weakness, and diarrhea (2). The abortion storms that occur in many livestock may be due to infection of the fetus or because of a reaction to the infection by the adult (2).

Currently no FDA approved vaccine or therapeutic exists to combat RVFV infection in humans. In some African countries (especially where the virus is endemic) outbreaks among livestock are contained using either inactivated or live attenuated vaccines (7). There are pros and cons for both types of vaccines. Inactivated vaccines are ideal from a biosafety standpoint because no live virus is present, but protective immunity may not be established from a single dose (7). This is problematic because the cost of providing vaccination and boosters could financially overwhelm many employers whose businesses rely on maintaining large livestock populations. Live attenuated vaccines can provide protective immunity after a single administration, but they are unsafe in both pregnant and young animals due to the live virus content (7). Three million doses of a newly developed live attenuated vaccine for livestock were recently distributed in South Africa, but no data as to the efficacy of the virus has been reported yet (7).

Because most human cases of RVFV are only mild infections that only cause general flu-like symptoms, no specific treatment is usually required (9). Because no licensed FDA vaccine

or approved therapeutic is available yet, the only treatment for severe RVFV infections in humans is supportive therapy (9). A recent study involving the ZH501 strain of RVFV, which is highly pathogenic, evaluated the activity of favipiravir against lethal subcutaneous infection in hamsters (10). Favipiravir is a possible candidate for treatment of RVFV infection. Favipiravir shows broad antiviral activity when used for treatment in many different RNA viruses (10). Normal subcutaneous infection in hamsters resulted in significant viral load accumulation in both the serum and tissues (10). Infections also lead to severe disease and death in hamsters two to three days post infection (10). Favipiravir administered orally to infected hamsters prevented mortality in at least sixty percent of the hamsters challenged (10). The only problem with favipiravir treatment of hamsters is that the oral administration must occur within one to six hours after exposure to be effective (10). In a more recent study conducted in 2014, Wistar Furth rats were exposed to aerosolized RVFV and favipiravir was tested as a treatment (17). It was determined from this study that administration of favipiravir up to 48 hours after infection demonstrated a significant reduction in mortality and length of progression to disease (17).

1.1.4 Public Health Significance

Rift Valley fever virus has the potential to affect the global economy as well as the health of the public throughout many countries. Considering the recent statistics indicating the upward trend of both the attack rate of the virus in humans and the mortality rates caused from those infections, an FDA approved therapeutic or vaccine may be essential to prevent the potential devastation caused by a future outbreak (6). RVFV can easily be transmitted through multiple mosquito genera, which dramatically increases the probability of the virus reaching naïve populations and establishing itself in the ecosystem (6). Recent data has also suggested that

RVFV possesses the ability to control its life cycle in the dominant mosquito species in a given region, which decreases the ability of any preexisting natural blockade to prevent the spread of the virus into naïve countries (12). Though differences in transmission rates exist between different genera of mosquitoes, the threat of eventual spread of RVFV to both Europe and the U.S. is very likely (6). Another unique attribute of RVFV is its ability to infect a broad range of hosts (6). Many viruses only have the ability to infect a limited host range, but RVFV has the potential to infect many hosts including: humans, goats, cattle, sheep, and other species (6). This potential to infect multiple species also increases the likelihood of the spread of RVFV to naïve populations.

Rift Valley fever virus also poses a significant threat to the health of the public from a bioterrorism standpoint. The Department of Health and Human Services and the Department of Agriculture both classify RVFV as an Overlap Select Agent in the United States (6). Not only is RVFV on the bioterrorism agent list of the Center for Disease Control, but it is also treated as a bio-threat through the US Commission on the Prevention of Weapons of Mass Destruction Proliferation and Terrorism (11) (6). These kinds of agents pose serious risks to national security and the health of the public due to their ease of dissemination and the potential to cause high rates of morbidity and mortality (12). RVFV has already been seriously considered as a potential bioweapon by the United States, and the offensive biological weapons program tested the virus in order to prove the reality that RVFV can be weaponized (12).

RVFV is also considered a serious zoonotic threat. A national policy established by the U.S Homeland Security already exists in order to defend the agriculture and food system of the United States from terrorist activity (6). After initial release (either intended or unintended) of RVFV into the United States or Europe, veterinarians and physicians would be generally

unaware of the clinical signs that RVFV presents leading to a delay of positive diagnosis in infected species (6). Sample handling and proper diagnostics available in Europe and the United States are limited for RVFV, which indicates that early detection and response time to any kind of attack or exposure would be unlikely until the virus was already well established (6). A RVFV outbreak or terrorist attack would also trigger an animal-trade embargo, which could detrimentally affect the economy of the target nation (6). International livestock trade has shifted RVFV many miles, but it also has the potential to possibly move various infected mosquito vectors to naïve countries (6). Based on these data, the conclusion drawn is that it is a question of when, not if, RVFV will be introduced (accidentally or purposefully) into Europe or the United States.

1.1.5 Animal Model

Rodents are versatile for many types of research based on the low cost to both purchase and house and also for their biological comparability to that of a human. This project involves the use of Lewis rats for all laboratory experiments. Previous research from our laboratory has demonstrated that different strains of rats exposed to RVFV elicit different clinical outcomes (13). Routes of exposure among various rat strains also determine the clinical outcome of infection (13). As depicted in Table 1 (shown below), Lewis rats demonstrate 100% mortality when exposed to RVFV via aerosol and 0% mortality when exposed via subcutaneous infection. We chose to use Lewis rats because they reflect the most reliable results through both infection routes. Mice also show more variation than Lewis rats between both routes of infection which is why we only chose to use Lewis rats (13). By understanding the various outcomes achieved from

both infection route and rat strain combination, our lab has developed a rat model that mimics clinical outcomes in people (13).

Table 1. Subcutaneous and aerosol infection routes in different rodent strains

		Subcutaneous		**Aerosol**	
Strain	**Dose (pfu)**	**Avg. % Mortality**	**Time to Death (days)**	**Avg. % Mortality**	**Time to Death (days)**
Wistar-Furth	10^3	90	3	100	4
ACI	10^3	10	15	100	6
Lewis	10^3	0	N/A	100	7

Table 1. Information: rat aerosol data from Bales et al. 2012 (13), and rat subcutaneous data from Peters and Slone 1982 (14).

As shown in the above table, neurological disease and subsequent death in Lewis rats is most consistent during aerosolization of RVFV. Signs of severe neurological disease that lead to euthanasia in Lewis rats include: seizures, loss of mobility, circling in caging, and uncontrollable rolling. Subcutaneous infection of RVFV in Lewis rats demonstrates no neurological disease or mortality. Knowing what route of infection is most likely to mimic severe disease in humans is important when considering initial model development (13). Treatment or prevention of the severe encephalitic form of the virus is still unknown due to the viral mechanisms utilized that enable infiltration and infection of the central nervous system (13). Therefore, aerosolization of RVFV in the Lewis rat model has proven to be the most consistent and useful in modeling and studying severe human infection (13).

Previous research conducted by the Hartman lab elucidated the pathogenesis of Rift Valley fever virus by using the Lewis rat model to detect specific biomarkers representative of

severe disease in Lewis rats (15). These experiments enabled a more holistic understanding of viral pathogenesis over the entire duration of infection.

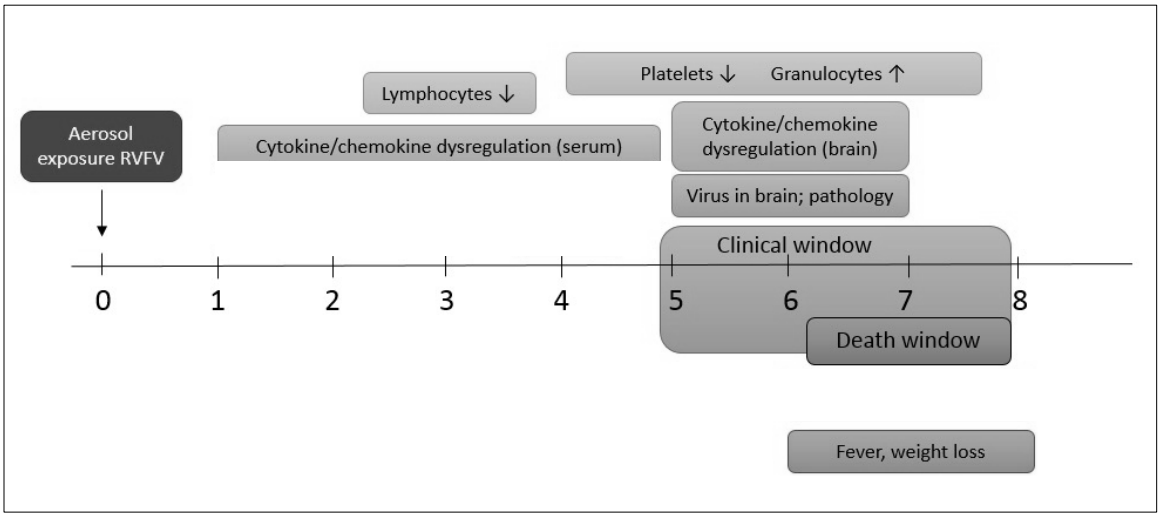

Figure 1. RVFV model of neurological disease in Lewis rats

Figure 1. Information: All data from Caroline et al. (2015) (15).

For the current research, the same Lewis rat model previously described was utilized in order to compare how viral infection progressed after administering virus via multiple routes of infection. The rat model was also used in order to attempt to quantify the distribution and location of viral infection throughout each day of infection, specifically infection progression in CNS tissues.

2.0 STATEMENT OF PROJECT AND SPECIFIC AIMS

2.1 PROJECT STATEMENT

Neurological disease caused by Rift Valley fever virus is poorly understood. Our lab uses a rat model that consistently displays lethal RVFV encephalitis, which involves aerosol infection of the animals. Subcutaneous infection of rats with the same virus does not cause illness or death except at very high doses. The goal of these studies was to better understand the disease in rats using different routes of RVFV infection. We chose to use aerosol, intranasal, and intratracheal routes of infection after developing our hypothesis that any virus deposited in the respiratory tract would lead to lethal encephalitis. We knew from previous aerosol infections that Lewis rats were sensitive to aerosol infection. We also wanted to test the differences between depositing viral particles in the lungs only (intratracheal infection), the nasal mucosa only (intranasal infection), and in both nasal mucosa and lungs (aerosol infection). We chose to test the intragastric route of infection to determine if successful infection by RVFV of the gastrointestinal tract could be initiated (naturally occurring via grooming). We chose to test the subcutaneous route of infection because it represents a natural route of infection (mosquitoes). It has also been historically shown that Lewis rats are resistant to subcutaneous infection with RVFV (13).

Using different routes of infection may provide valuable insight that contributes to our understanding of the pathogenesis of the virus and how the clinical outcome in animals may vary based on the type of tissue within the body where virus first makes contact. Determining if CNS vascular leakage occurs in rats that die of encephalitis may also lead to future studies demonstrating whether virus travels to different parts of the body via the bloodstream.

2.2 PROJECT AIMS

Specific Aim 1: To determine the clinical outcome of rats infected with virulent Rift Valley fever virus using alternate routes of infection. Our research on Rift Valley fever virus focused primarily on aerosol infections in the past, so we have little insight as to whether alternate routes of infection change the outcome of disease progression. We hypothesized that routes of infection that deposit virus into the respiratory tract (intratracheal, and intranasal) would lead to encephalitis and death comparable to aerosol infection. We expected that the intragastric route of infection would not lead to severe disease and would demonstrate a clinical outcome comparable to subcutaneous infection.

1. We compared survival, weight loss, and body temperature of rats infected with RVFV by multiple infection routes including: aerosol, intranasal, intratracheal, subcutaneous, and intragastric.
2. Compared the spread of virus through the CNS
3. Compared changes in blood cell counts in rats infected by aerosol and subcutaneous routes

Specific Aim 2: To measure the vascular integrity of the brain in Rift Valley fever infected rats to determine if/when breakdown of the blood brain barrier occurs. We hypothesized that vascular leakage would occur in the brain either just before or during the onset of clinical signs. We tested this hypothesis by measuring the amount of vascular leakage that occurred using a sodium fluorescein assay and IVIS imaging.

1. The amount of vasculature leakage that occurred in Rift Valley fever infected rats was visualized and quantified using both IVIS imaging and leakage of FITC salt.

3.0 METHODS AND MATERIALS

3.1 ANIMAL INFORMATION

Female Lewis Rats (Envigo: 1706F) were used for all studies. The rats were 8-10 weeks old and weighed 150-174g on average. Rats used in imaging studies were given alfalfa free chow (Harlan: 2914-122115M) in order to decrease the amount of autofluorescence and to improve the overall quality of image acquisition. IACUC animal protocol numbers used in the studies were 14125012 and 15076006. Infected rats were monitored once daily until they reached a certain threshold of sickness in which case they were monitored twice daily. Temperature chips (BMDS: IPTT-300) were implanted before infection in order to obtain baseline data and maintain temperature readings throughout the experiments.

3.2 VIRUS INFORMATION

All RVFV infections utilized the same strain of virus, ZH501. The wild type ZH501 virus was originally isolated from a patient during the Egyptian RVFV outbreak in 1977. This strain of RVFV was provided by Barry Miller (CDC, Fort Collins, Colorado) and Stuart Nichol (CDC, Atlanta, Georgia). The virus was then propagated on VeroE6 cells prior to infection. All work with live virus was performed in a BSL-3 laboratory at the Regional Biocontainment Laboratory

(RBL). All personnel were required to don powered air purifying respirators (3M Versaflo PAPR unit TR-300N) when working in the BSL-3 laboratory. All live virus sample work was conducted in a class II biological safety cabinet. All waste was autoclaved before removal from the facility. All surfaces were disinfected using Vesphene II se (Steris Corp., Erie, Pennsylvania). The RBL at the University of Pittsburgh is registered with the CDC/USDA for all work with RVFV.

3.3 TEMPERATURE TRANSPONDER IMPLANT PROCEDURE

Before each RVFV viral inoculation took place, implantable electronic ID transponders (BMDS, Seaford, Delaware) were utilized for temperature data acquisition throughout the course of each experiment. Rats were first anesthetized using Isothesia (Isoflurane, USP NDC 11695-0500-2) in a drop container. The temperature transponder was then injected subcutaneously between the shoulder blades of each rat. Temperature acquisition was then maintained throughout each experiment by reading each animal's temperature transponder.

3.4 AEROSOL INFECTION

Dr. Douglas Reed and his lab members performed all aerosol infections for the current research. All aerosols involved exposing Lewis rats to the virulent ZH501 strain of Rift Valley fever virus with a target dose of 3×10^4 pfu. Rats were exposed to virus in a class III biosafety cabinet using a Collision 3-jet or Aeroneb nebulizer in a whole body chamber. Aerosol samples

were collected using an all-glass impinger to determine aerosol concentration. After the aerosols were performed, rats were returned to their cages and monitored in the RBL for signs and symptoms of infection. Presented aerosol dose was calculated using a previously described method (16). Virus concentration in the nebulizer and impinger for each aerosol were determined through plaque assay (16). The presented dose each aerosol was then calculated by first obtaining the respiratory minute volume, which was determined using Guyton's formula (16). By multiplying the respiratory minute volume by the length of the aerosol exposure, the total inhaled volume could be calculated (16). By multiplying the total inhaled volume by the concentration of the aerosol (determined from the initial plaque assay), the presented aerosol dose could be obtained. (16)

3.5 INTRATRACHEAL INFECTION

We used 1ml syringes with feeding needles to administer 200ul of 2×10^4 pfu of virulent ZH501 Rift Valley fever virus directly into the lungs of Lewis rats. Rats were first exposed to Isothesia (Isoflurane, USP NDC 11695-0500-2) in a drop container to induce general anesthesia. The feeding needle was then inserted into the trachea (accessed after first entering the esophagus and penetrating the epiglottis) and the syringe content was then released into the lungs.

3.6 INTRAGASTRIC INFECTION

We used 1 ml syringes with feeding needles to administer 200ul of 2 x 10^5 pfu of virulent ZH501 Rift Valley fever virus directly into the stomachs of Lewis rats. Rats were first exposed to Isothesia (Isoflurane, USP NDC 11695-0500-2) in a drop container to induce general anesthesia. The feeding needle was then inserted into the esophagus (without penetrating the epiglottis as in intratracheal infection) and the syringe content was then released into the stomach.

3.7 INTRANSAL INFECTION

Rainin 200ul Pipets (BO812865K) were used to administer 200ul of 2 x 10^4 pfu of virulent ZH501 Rift Valley fever virus directly to the nostrils of Lewis rats. Rats were first exposed to Isothesia (Isoflurane, USP NDC 11695-0500-2) in a drop container to induce general anesthesia. The viral dilution was then applied equally to each nostril of the Lewis rats.

3.8 SUBCUTANEOUS INFECTION

We used ½ cc Lo-Dose Insulin Syringes with 28-½ gauge needles to administer 500ul of 1 x 10^6 pfu of virulent ZH501 Rift Valley fever virus subcutaneously (under the skin) to the hind legs of Lewis rats. Rats were first exposed to Isothesia (Isoflurane, USP NDC 11695-0500-2) in

a drop container to induce general anesthesia. The predetermined viral dilution was then injected subcutaneously into the right hind leg of the Lewis rats.

3.9 RNA EXTRACTION AND RT - PCR

All tissue and serum samples used for PCR analysis were initially inactivated using a previously tested method approved by the University of Pittsburgh's RBL Biosafety Officer. This inactivation step of the samples is important to ensure that virus was inactivated prior to transport to the BSL II environment. 900ul of Trizol reagent was first added to 2.0ml Eppendorf tubes. 100ul of infectious sample was then added to each Eppendorf tube. The sample/Trizol mixtures were then inverted continuously for thirty seconds and allowed to rest for five minutes. Samples were then transferred to new previously labeled storage tubes and brought out of containment. The samples were then stored frozen until RNA extraction could be run. 200ul of chloroform was then added to each sample and spun at 12,000 x g for 15 min. The aqueous phase was then removed and used for extraction. The completely inactivated RNA was then extracted using a PureLink RNA Mini Kit (Ambion 12183025) for tissue samples, or a PureLink Viral RNA/DNA Kit (Invitrogen 12280-50) for serum samples. These kits utilize a spin column method in order to filter out viral RNA. Once viral RNA was isolated following the respective protocol for either tissue or serum samples, a SuperScript III Platinum One-Step Quantitative RT-PCR Kit (Invitrogen 11745-500) was used in order to amplify each RNA sample. Results were compared to a standard curve that was generated from 10-fold RVFV RNA dilutions from stock with a known titer.

3.10 IVIS IMAGING

All imaging took place in the RBL at the University of Pittsburgh using a Spectrum CT In Vivo Imaging System (IVIS; Perkin Elmer). Rats were first infected using the aerosol route performed by Dr. Douglas Reed. Rats were then serially imaged 3-7 days post infection. On each day of imaging, the rats were exposed to either ketamine/xylazine or prolonged isoflurane for proper anesthetization. Multiple fluorescent agents were used during the different studies (Superhance 680 – Perkin Elmer, FITC Salt – Sigma Aldrich). Reagents were injected into the tail veins of the rats and allowed to circulate for an amount of time indicated by the manufacturer. Rats were then placed into the IVIS chamber for imaging. The IVIS machine was calibrated prior to each study using the emission and excitation settings provided by each reagents manufacturer. After image acquisition, Living Image Software 4.5.2 (PerkinElmer) was used for analysis.

3.11 CBC AND BLOOD CHEMISTRY

Rat blood samples were analyzed immediately after animal euthanasia. Samples were tested on both the Abaxis Vetscan HM2 Hematology Blood Analyzer and the Abaxis Vetscan VS2 Veterinary Blood Chemistry Analyzer. The HM2 analyzer provided us with information regarding the types of cells in the blood and exactly how many were present. The types of cells specifically quantified were white blood cells, platelets, and red blood cells. The VS2 analyzer provided us with information regarding blood chemistry, electrolytes, and blood gases. Vacutainer tubes (BD 367841) with K2 EDTA anticoagulant were used to collect blood samples

for HM2 blood analysis. Vacutainer tubes (BD 366664) with Lithium Heparin anticoagulant were used to collect blood samples for VS2 blood analysis. VetScan Comprehensive Diagnostic Profile Reagent Rotors (Abaxis 500-7123) were used in conjunction with the VS2 blood analyzer to quantify blood chemistry results.

4.0 RESULTS

4.1 AIM 1: TO DETERMINE THE CLINICAL OUTCOME OF RATS INFECTED WITH VIRULENT RIFT VALLEY FEVER VIRUS USING ALTERNATE ROUTES OF INFECTION

The initial technique used in examination of the differences between all previously described routes of Rift Valley fever virus infection in rats was to compare their survival curves. By plotting survival curves acquired from each route of infection, a comparison of the lethality of RVFV based on the administration route could be better understood. This also provided a comparison of the speed of disease onset among the various routes of infection (Figure 2).

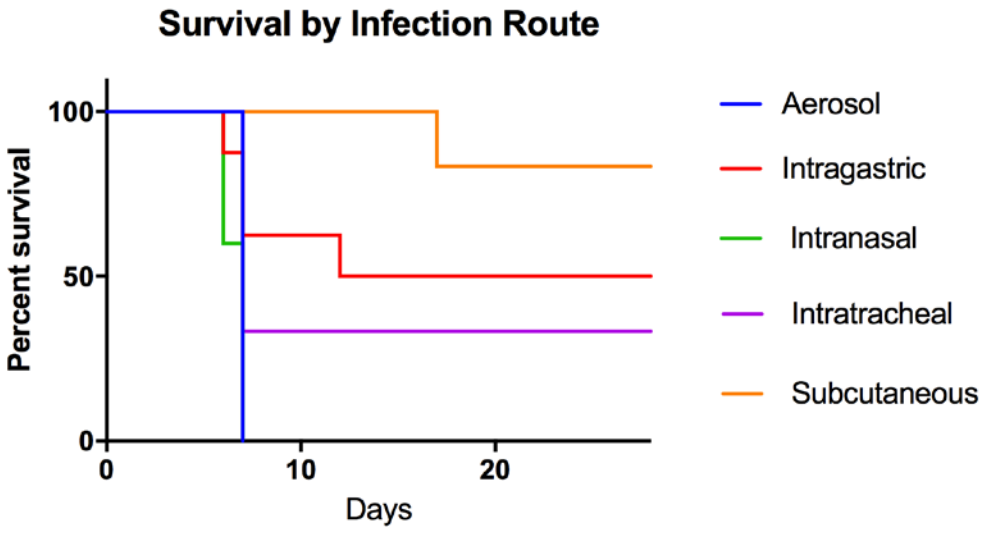

Figure 2. Survival curves

Kaplan Meier survival plot comparing all infection routes and doses tested using RVFV. Five different cohorts of rats were infected with RVFV using various routes of infection. The doses administered for each route are as follows: Aerosol – 2.1 x 10^3 pfu/ml, Intragastric – 2.0 x 10^5 pfu/ml, Intranasal – 2.0 x 10^4 pfu/ml, Intratracheal – 2.0 x 10^4 pfu/ml, Subcutaneous – 1.0 x 10^6 pfu/ml. It is important to note that the intranasal survival curve follows the aerosol survival curve.

Each group of rats was monitored daily for signs of illness using approved IACUC scoring criteria. Rats were euthanized when moribund based on these scoring criteria although most were euthanized based on the severity of neurological signs as had been previously determined (13). Signs of severe neurological disease that lead to euthanasia in Lewis rats include: seizures, loss of mobility, circling in caging, and uncontrollable rolling. Based on the data from survival curves from each infection route, rats infected through the intranasal and aerosol routes progressed most quickly to death with 100% mortality in both groups. Intragastric and intratracheal inoculations established a lower amount of infection but still reached between

50% - 60% mortality. Subcutaneous infection caused the lowest mortality rate (20%) and many rats displayed no signs or symptoms of any kind of infection.

In addition to comparing survival, clinical signs of disease (temperature and weight loss) were monitored and compared between the different routes of inoculation. (Figures 3-7)

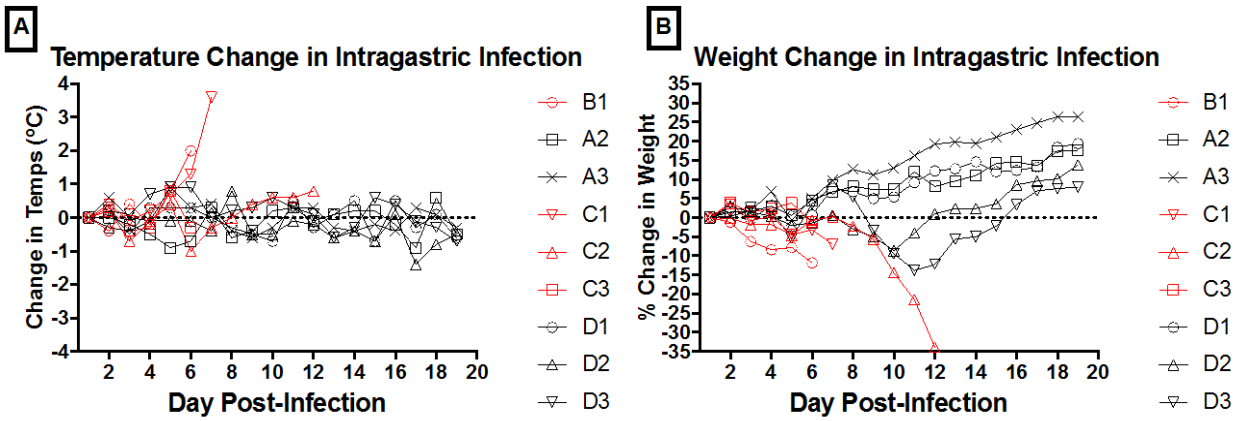

Figure 3. Comparison of body temperature and weight change in Lewis rats infected via intragastric instillation

Nine female Lewis rats were infected intragastrically with RVFV 2.0 x 10^5 pfu/animal in order to determine the effect of this type of infection route. The rats were monitored for disease progression using daily body temperature (A) and weight (B) measurements. The rats were also monitored visually for any development of signs of infection commonly associated with RVFV. Red highlighted subjects indicate progression of the disease to the point of euthanasia.

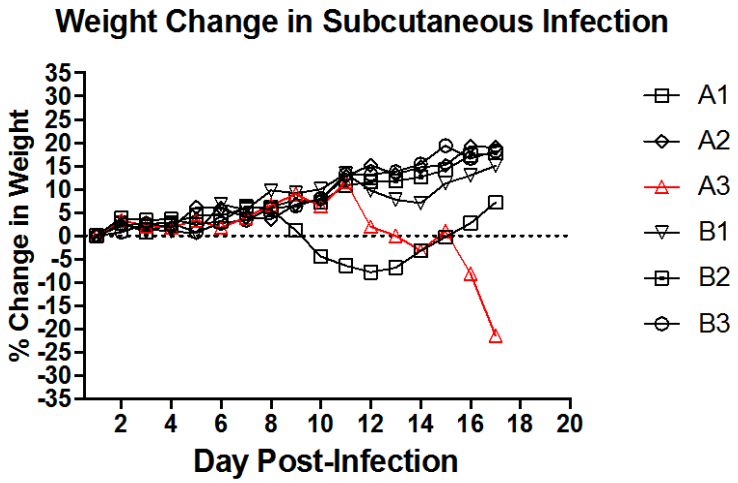

Figure 4. Weight change in Lewis rats infected subcutaneously

Six female Lewis rats were infected via the subcutaneous route with RVFV 1.0 x 10^6 pfu/animal in order to determine the effect of this type of infection route. The rats were monitored for disease progression using daily weight measurements. The rats were also monitored visually for any development of signs of infection commonly associated with RVFV. Red highlighted subjects indicate progression of the disease to the point of euthanasia.

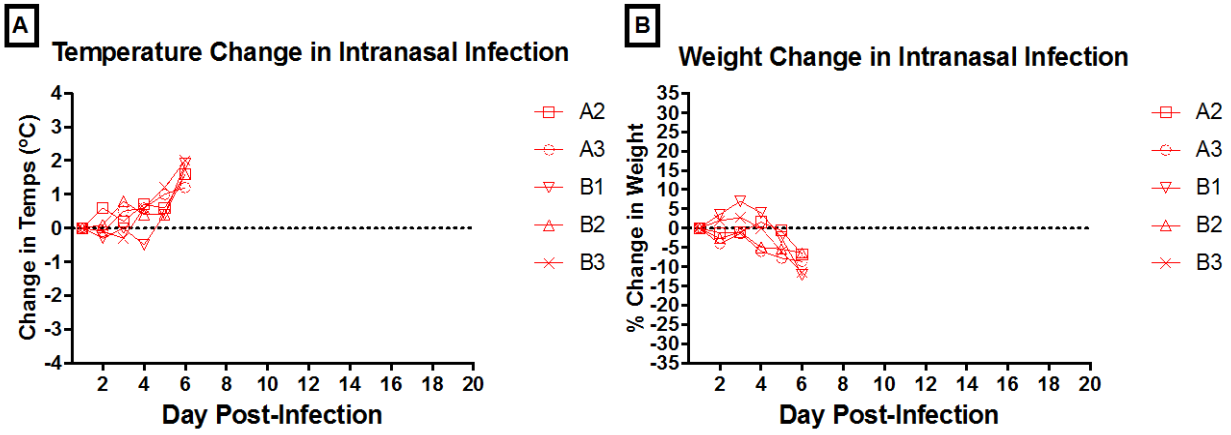

Figure 5. Comparison of body temperature and weight change in Lewis rats infected via intranasal instillation

Five female Lewis rats were infected intranasally with RVFV 2.0 x 10^4 pfu/animal in order to determine the effect of this type of infection route. The rats were monitored for disease progression using daily body temperature (A) and weight (B) measurements. The rats were also monitored visually for any development of signs of infection commonly associated with RVFV. Red highlighted subjects indicate progression of the disease to the point of euthanasia.

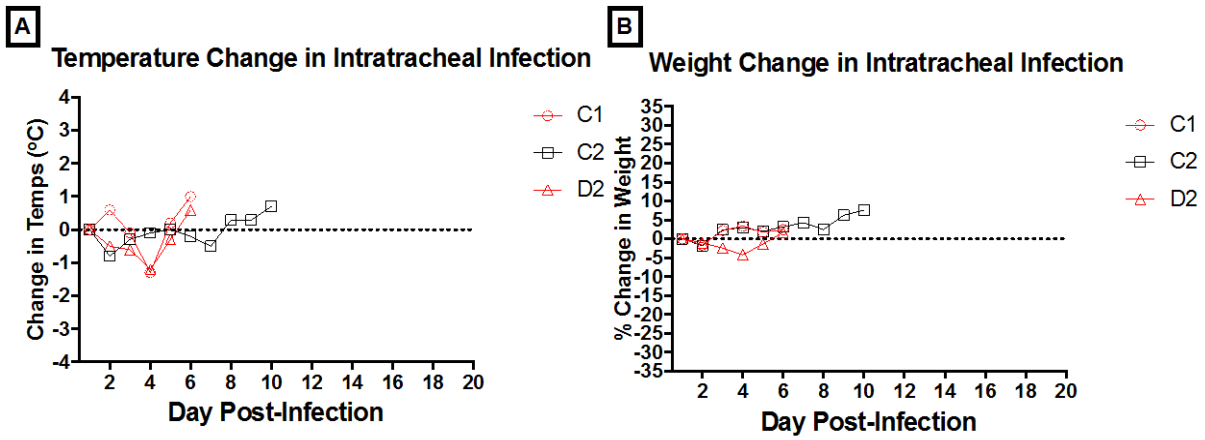

Figure 6. Comparison of body temperature and weight change in Lewis rats infected via intratracheal instillation

Three female Lewis rats were infected intratracheally with RVFV 2.0 x 10^4 pfu/animal in order to determine the effect of this type of infection route. The rats were monitored for disease progression using daily body temperature (A) and weight (B) measurements. The rats were also monitored visually for any development of signs of infection commonly associated with RVFV. Red highlighted subjects indicate progression of the disease to the point of euthanasia.

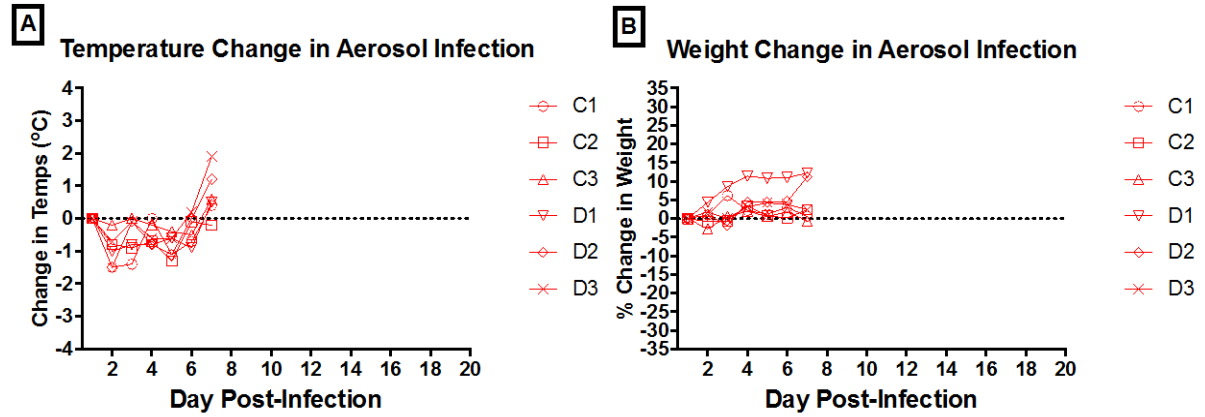

Figure 7. Comparison of body temperature and weight change in Lewis rats infected via aerosol exposure

Six female Lewis rats were infected via aerosol with RVFV 2.1 x 10^3 pfu/animal in order to determine the effect of this type of infection route. The rats were monitored for disease progression using daily body temperature (A) and weight (B) measurements. The rats were also monitored visually for any development of signs of infection commonly associated with RVFV. Red highlighted subjects indicate progression of the disease to the point of euthanasia.

Based on the temperature data acquired from the rats infected intragastrically (Figure 3), only two of the four animals that were euthanized developed a fever based on the approved scoring system. Interestingly, three of the four animals displayed at least five percent weight loss before euthanasia. Three of the four animals that were euthanized all developed severe infection during the previously established clinical window. The other animal did not begin to lose weight or develop a temperature until 10DPI (three days after the normal clinical window). All other animals maintained normal temperatures and weights throughout the duration of the experiment. Subcutaneously infected rats (Figure 4) were only monitored for changes in weight. Temperature chips were not implanted before infection during this experiment. Based on the weight data acquired, two animals displayed at least ten percent weight loss (beginning between 10 and 12DPI). Only one of the animals was euthanized based on other neurological criteria while the other animal successfully recovered from infection. All other animals slowly gained weight over the course of the experiment. Intranasally infected rats (Figure 5) were monitored for changes in both temperature and weight. All five animals developed fevers and displayed weight loss between five and ten percent. All animals were euthanized during the previously established clinical window for RVFV infection in Lewis rats (5-7DPI). Intratracheally infected rats (Figure 6) were also monitored for changes in both temperature and weight. Only two of the three rats infected reached the criteria for euthanasia. Both of these animals did not experience any weight change from baseline until the time of euthanasia (6DPI). It appeared from the data that the onset of fever was beginning, but other neurological symptoms caused euthanasia before full onset of fever. The other animal did not develop any symptoms and survived intratracheal infection. Aerosol infected rats (Figure 7) were monitored for changes in both temperature and weight. All six of the rats infected reached criteria for euthanasia. Only two of the six animals developed

fevers before euthanasia and no animals lost weight during the course of the experiment. All animals developed neurological symptoms that lead to euthanasia during the clinical window (5-7DPI).

We next wanted to examine the differences in viral load in tissues and blood samples harvested from rats inoculated with Rift Valley fever virus using the previously described routes of infection. This comparison between infection routes provided information regarding viral migration after the initial site of viral administration. PCR analysis was used to quantify the viral load present in each respective tissue and serum sample from the previously described experimental infection routes (Figures 8-10).

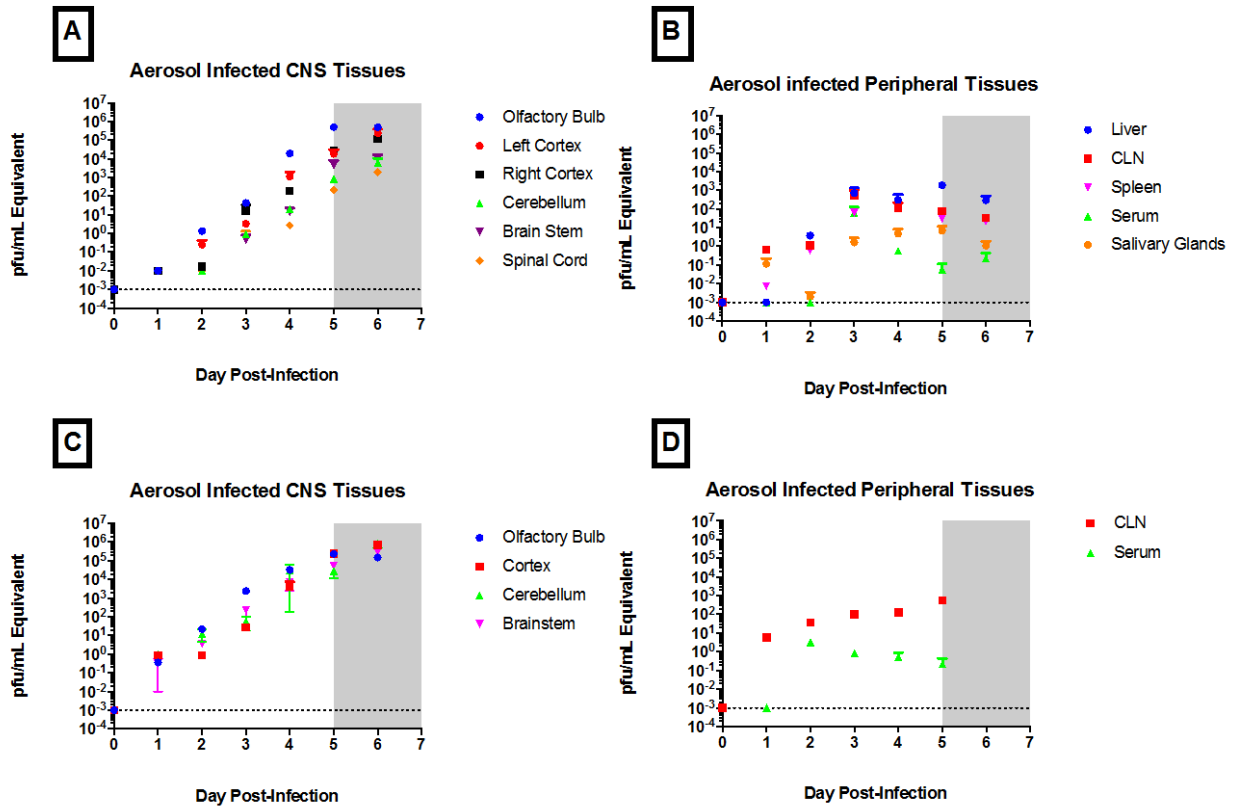

Figure 8. PCR data from Lewis rats exposed to aerosolized RVFV

In (A) and (B) 18 female Lewis rats received an aerosolized dose of Rift Valley fever virus at 1.0 x 10^3 pfu/animal. In (C) and (D) 21 rats received an aerosolized dose of Rift Valley fever virus at 2.0 x 10^4

pfu/animal. Rats from both experiments were then serially sacrificed on the corresponding days. Tissues were collected and viral titer was determined using PCR.

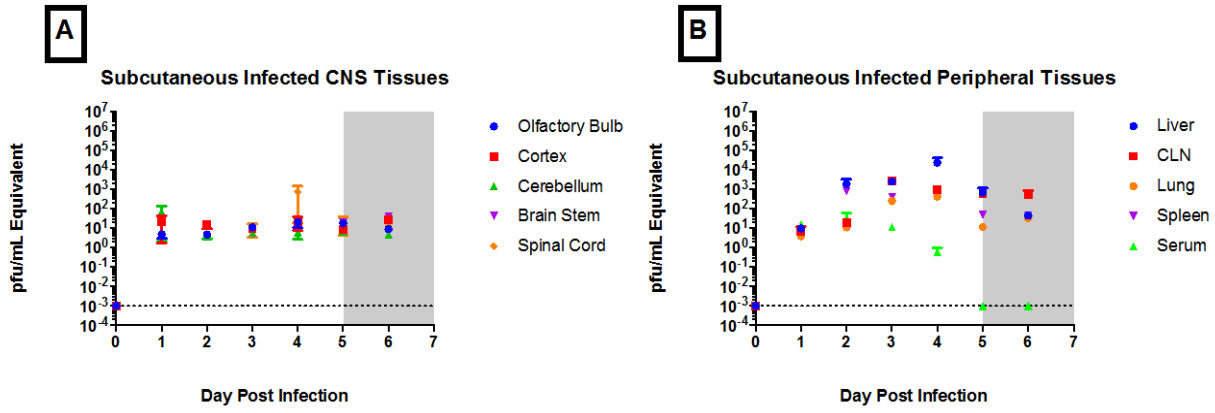

Figure 9. PCR data from Lewis rats exposed to RVFV via subcutaneous instillation

12 female Lewis rats received a subcutaneous dose of Rift Valley fever virus at 1.0 x 10^6 pfu/animal. They were then serially sacrificed on the corresponding days. Tissues were collected and viral titer was determined using PCR.

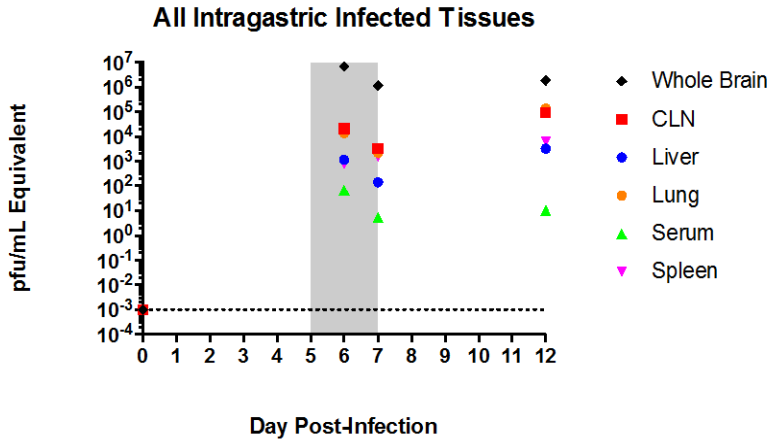

Figure 10. PCR data from Lewis rats exposed to RVFV via intragastric instillation

Nine female Lewis rats received an intragastric dose of Rift Valley fever virus at 2.0 x 10^5 pfu/animal. They were then euthanized on the corresponding days due to infection. Tissues were collected and viral titer was determined using PCR.

Tissues analyzed from aerosol infection routes (Figure 8) showed elevated viral load in CNS tissues, including the olfactory bulb, cortex, cerebellum, brainstem, and spinal cord. The elevated viral load in CNS tissues began 3-4DPI (1×10^3 pfu/ml – 1×10^4 pfu/ml) and increased until euthanasia (1×10^6 pfu/ml). Peripheral organs such as the liver, cervical lymph nodes, and spleen maintained lower viral load throughout the duration of the experiment (1×10^2 pfu/ml – 1×10^3 pfu/ml). The viral load in tissues analyzed from subcutaneous infection (Figure 9) was elevated in tissues such as the liver, spleen, cervical lymph nodes, and lungs beginning 2DPI (1×10^3 pfu/ml) and extending through 4DPI (1×10^4 pfu/ml), compared to subcutaneous infected brain tissues that remained consistently low throughout infection. CNS tissues maintained low viral load throughout the duration of the experiment (1×10^1 pfu/ml – 1×10^2 pfu/ml). Tissues analyzed from intragastric infection (Figure 10) also displayed highest viral loads in CNS tissues beginning on 6DPI (1×10^7 pfu/ml) extending out until 12DPI (1×10^6 pfu/ml). Peripheral organs also had elevated levels of virus especially in the cervical lymph nodes and lungs (6DPI 1×10^4 pfu/ml – 12DPI 1×10^5 pfu/ml).

In order to further understand the pathogenesis of the virus and the immune response generated by RVFV infection, the Abaxis Vetscan HM2 Hematology Blood Analyzer (HM2) was used. This allowed us to obtain information regarding the types of cells in the blood and exactly how many were present by testing whole blood samples treated with EDTA from each animal. The types of cells specifically quantified were white blood cells, platelets, and red blood cells.

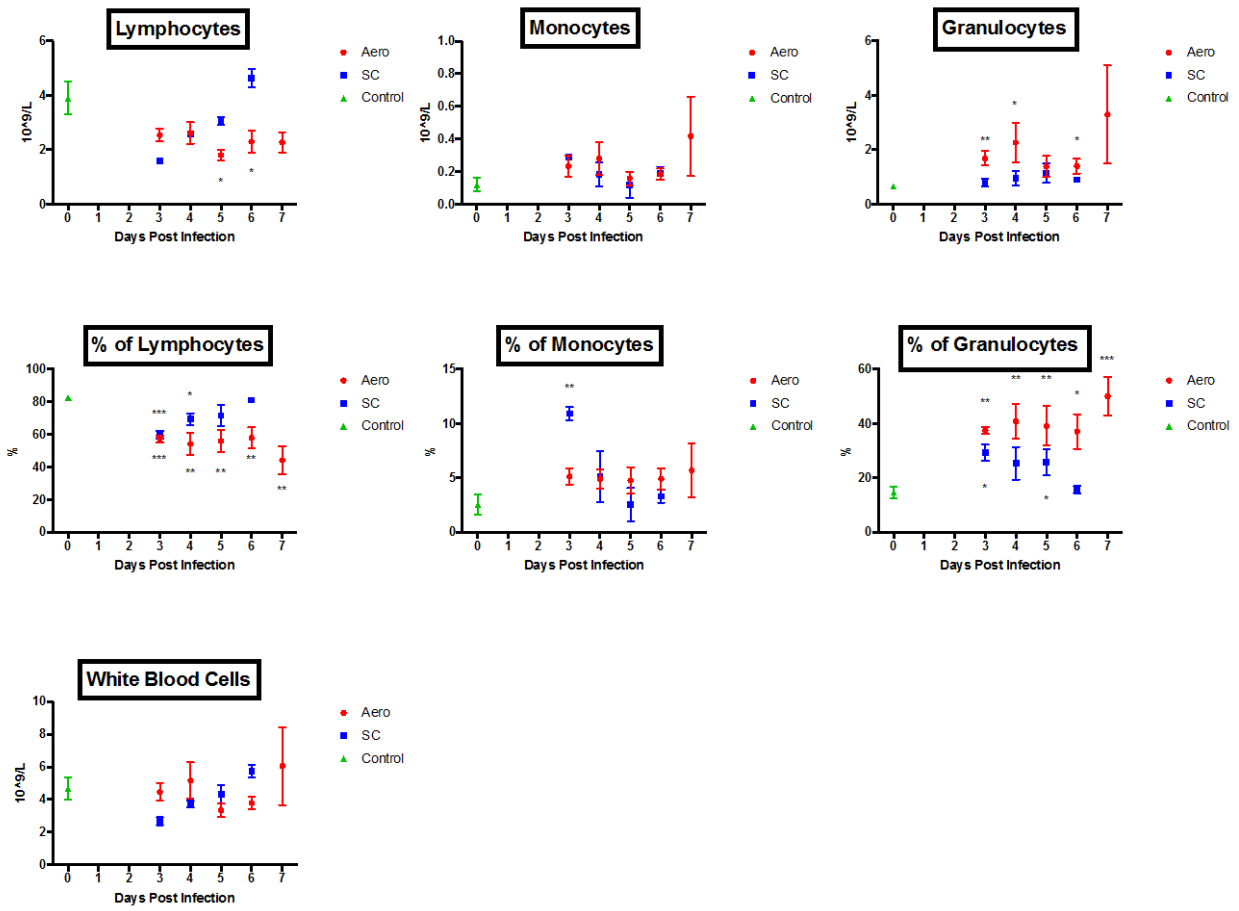

Figure 11. Complete blood counts (CBC) from aerosol, subcutaneous, and control Lewis rats

Female Lewis rats were infected by either aerosolization (2.1 x 10^3 pfu/animal), subcutaneous instillation (1.0 x 10^6 pfu/animal), or were uninfected for control. Infected animals were serially sacrificed from 3DPI to 7DPI. Whole blood samples were collected in 2ml vacutainer tubes with EDTA as anticoagulant. Blood samples were then run on the Abaxis Vetscan HM2 Hematology Blood Analyzer. An asterisk (*) above or below a point indicates the level of significance determined by an unpaired t-test between that value and the control value. Asterisks indicate significance as follows: ****=p<0.0001; ***=0.0001<p<0.001; **=0.001<p<0.01; *=0.01<p<0.05.

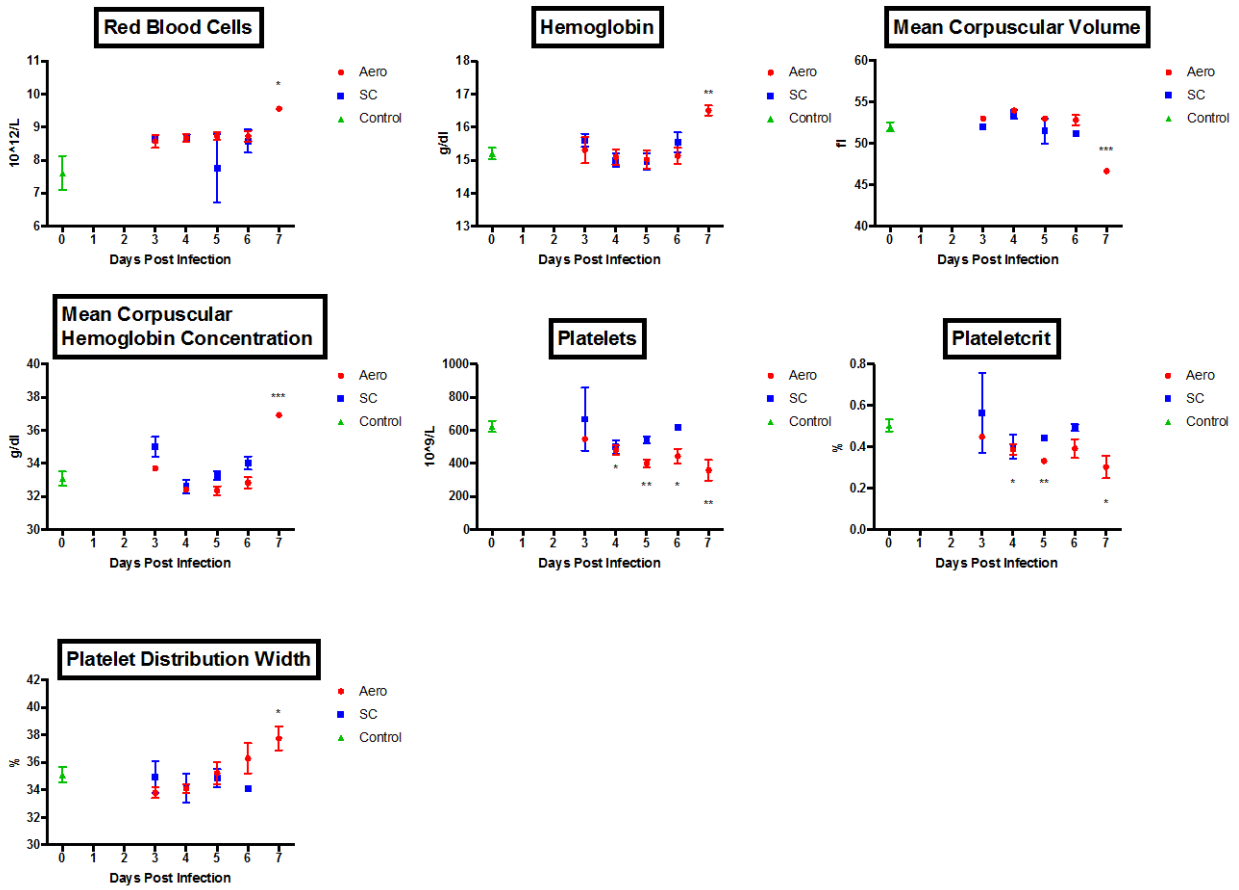

Figure 12. Red blood cell and platelet counts from aerosol, subcutaneous, and control Lewis rats

Female Lewis rats were infected by either aerosolization (2.1 x 10^3 pfu/animal), subcutaneous instillation (1.0 x 10^6 pfu/animal), or were uninfected for control. Infected animals were serially sacrificed from 3DPI to 7DPI. Whole blood samples were collected in 2ml vacutainer tubes with EDTA as anticoagulant. Blood samples were then run on the Abaxis Vetscan HM2 Hematology Blood Analyzer. An asterisk (*) above or below a point indicates the level of significance determined by an unpaired t-test between that value and the control value. Asterisks indicate significance as follows: ****=p<0.0001; ***=0.0001<p<0.001; **=0.001<p<0.01; *=0.01<p<0.05.

Blood analyzed from aerosol infection, subcutaneous infection, and control Lewis rats was used to determine levels of white blood cells counts, lymphocyte counts, monocyte counts, and granulocyte counts (Figure 11). The level of significance for all infection route time points was determined by using an unpaired t-test comparing each infection route time point to the control value in each panel. White blood cell levels (WBC) in both aerosol and subcutaneous

infected animals displayed no significant difference ($p>0.05$) from control animals white blood cell counts throughout the duration of the experiment. Lymphocyte levels (LYM) in blood samples from aerosol infected rats remained low from 3DPI – 7DPI and were significantly lower than control lymphocyte levels on both 5DPI ($p<0.05$) and 6DPI ($p<0.05$). Lymphocyte levels in blood samples from subcutaneous infected rats appeared visually lower than control levels on 3DPI although this difference was not significant ($p>0.05$). Monocyte levels (MON) in both aerosol and subcutaneous infected animals matched control monocyte levels throughout the duration of the experiment with no significant differences ($p>0.05$). Granulocyte levels (GRA) in aerosol infected animals tended to be higher than control granulocyte levels and were significantly higher on 3DPI ($p<0.05$), 4DPI ($p<0.05$), and 6DPI ($p<0.05$). Granulocyte levels in subcutaneous infected animals matched control granulocyte levels throughout the duration of the experiment with no significant differences ($p>0.05$). From these results, there was lymphocytopenia and granulocytosis in aerosol infected rats, but not in subcutaneous infected rats. These results coincide with our previously established Lewis rat model.

Blood analyzed from aerosol infection, subcutaneous infection, and control Lewis rats was also used to analyze red blood cell counts and to determine information regarding platelet content and distribution (Figure 12). Red blood cell levels (RBC) in aerosol infected animals were not significantly different ($p>0.05$) than control levels until 7DPI ($p<0.05$) when they became significantly higher than control values. Red blood cell levels in subcutaneous infected animals were not significantly different ($p>0.05$) than control values throughout the duration of the experiment. Similarly, the measurement of hemoglobin (HGB) in aerosol and subcutaneous infected animals was not significantly different ($p>0.05$) than control levels throughout the duration of the experiment until 7DPI ($p<0.05$) when levels in aerosol infected animals became

significantly higher than control values. The measurement of mean corpuscular volume (MCV) in aerosol and subcutaneous infected animals was not significantly different ($p>0.05$) than control levels throughout the duration of the experiment until 7DPI ($p<0.05$) when levels in aerosol infected animals became significantly lower than control values. The measurement of mean corpuscular hemoglobin concentration (MCHC) in aerosol and subcutaneous infected animals was not significantly different ($p>0.05$) than control levels throughout the duration of the experiment until 7DPI ($p<0.05$) when levels in aerosol infected animals became significantly higher than control values. Platelet counts (PLT) in aerosol infected animals were significantly lower than control levels on 4DPI ($p<0.05$), 5DPI ($p<0.05$), 6DPI ($p<0.05$), and 7DPI ($p<0.05$). Platelet counts in subcutaneous infected animals matched control levels throughout the duration of the experiment with no significant differences ($p>0.05$). The plateletcrit (PCT) in aerosol infected animals was significantly lower than control levels on 4DPI ($p<0.05$), 5DPI ($p<0.05$), and 7DPI ($p<0.05$). The plateletcrit in subcutaneous infected animals matched the control plateletcrit throughout the duration of the experiment with no significant differences ($p>0.05$). The platelet distribution width (PDWc) reflects how uniform platelets are in size. The PDWc in aerosol infected animals was not significantly different ($p>0.05$) than control levels until 7DPI ($p<0.05$) when platelet distribution width became significantly higher than control values. This variation in platelet size may have been caused by the production of new platelets by bone marrow (smaller sized platelets) in response to overall platelet death on 7DPI caused by viral infection in aerosol infected animals. Platelet distribution width in subcutaneous infected animals matched control values throughout the duration of the experiment with no significant differences ($p>0.05$). From these results, there was clear thrombocytopenia in aerosol infected rats, but not in

subcutaneous infected rats. These results coincide with our previously established Lewis rat model.

4.2 AIM 2: TO MEASURE THE VASCULAR INTEGRITY OF THE BRAIN IN RIFT VALLEY FEVER INFECTED RATS TO DETERMINE IF/WHEN BREAKDOWN OF THE BLOOD BRAIN BARRIER OCCURS.

Next we wanted to determine whether the blood brain barrier breaks down after RVFV infection and whether this breakdown occurs before or after virus reaches the brain. To do this, we visualized and quantified the amount of vascular leakage that occurred in Rift Valley fever infected Lewis rats using a Spectrum CT In Vivo Imaging System (IVIS). Rats were first infected using the aerosol route as described in the methods section. Rats were then serially imaged 3-7 days post infection. On each day of imaging, the rats were first anesthetized before imaging agent (Superhance 680 – Perkin Elmer – Molecular Weight = 1540) was injected into the tail vein and allowed to circulate. This imaging agent is able to pass through small breaks in the vasculature of the blood brain barrier and access the central nervous system. Rats were then placed into the IVIS chamber for imaging to determine the amount of vascular breakdown. The IVIS machine was calibrated prior to each study using the emission and excitation settings provided by the manufacturer. After image acquisition, Living Image Software 4.5.2 (PerkinElmer) was used for analysis.

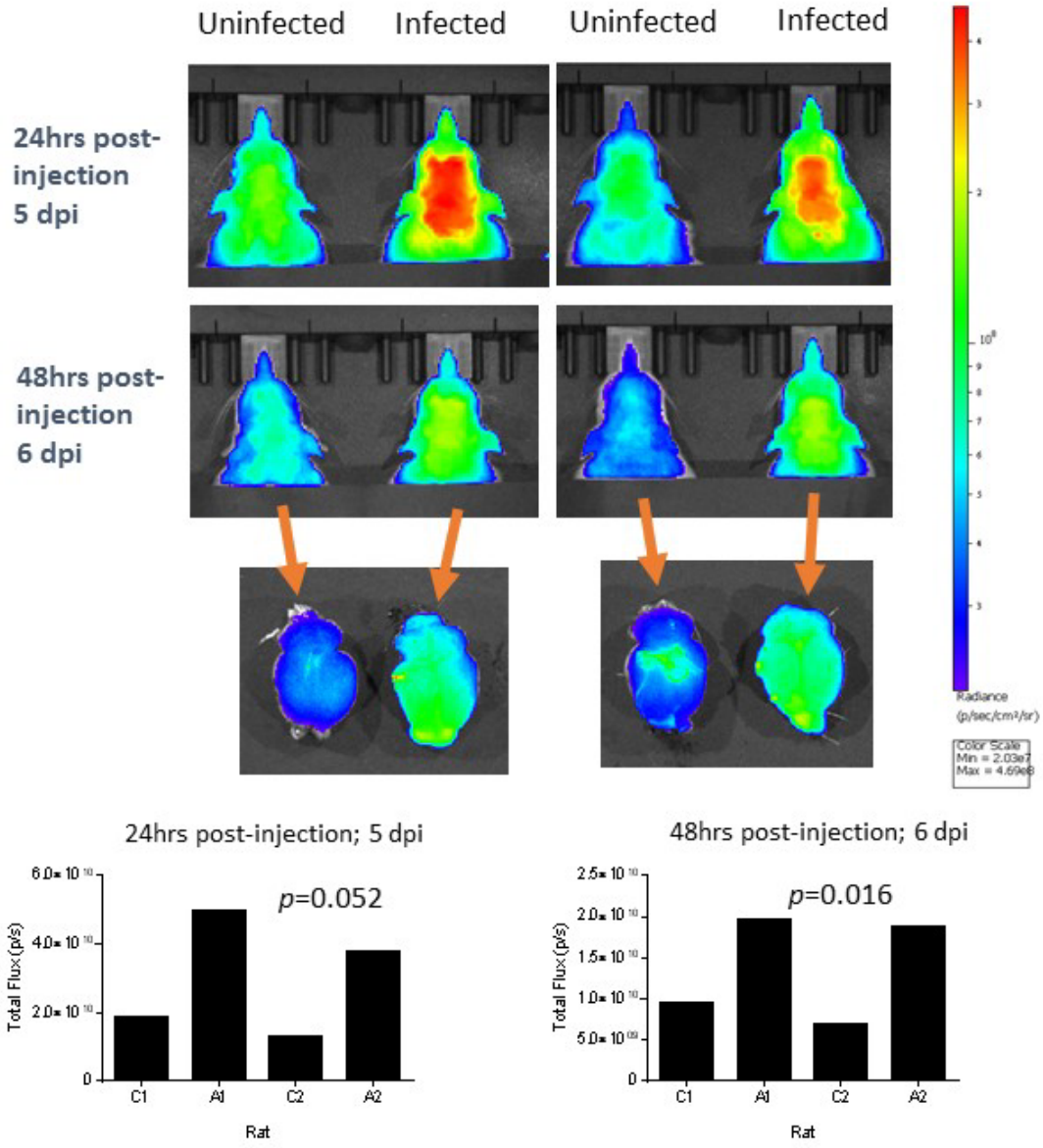

Figure 13. Vascular integrity determined by Spectrum CT in Vivo Imaging System (IVIS)

Superhance 680, a small fluorescent *in vivo* blood pool-imaging agent (MW = 1540) was injected into rats 4 days after RVFV aerosol infection. Rats were then imaged 24 and 48 hours later to observe vascular leakage in uninfected vs. infected rats. At 48 hours post injection (=6 dpi), the brains were removed for *ex vivo* imaging. Total flux represents the intensity of the agent in the tissue observed.

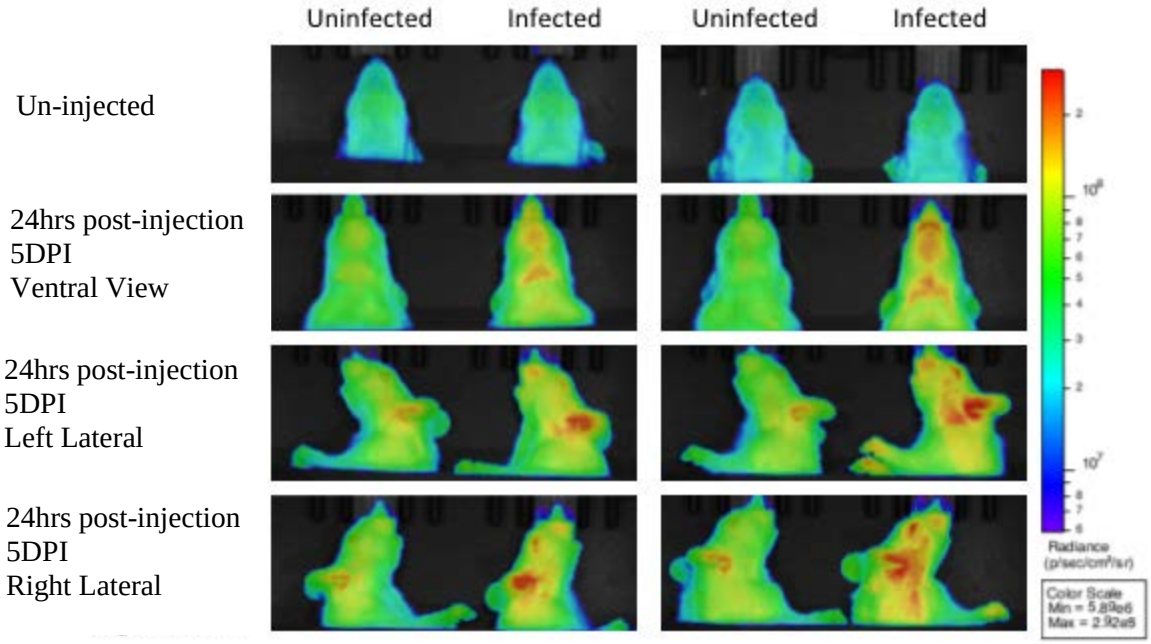

Figure 14. Multiple IVIS angles confirming vascular leakage in uninfected vs. infected animals

Superhance 680, a small fluorescent *in vivo* blood pool-imaging agent (MW = 1540) was injected into rats 4 days after RVFV aerosol infection. Rats were then imaged 24 hours later to observe vascular leakage in uninfected vs. infected rats. Rats were manipulated between images to achieve the desired angle during imaging. All imaging conditions were the same between pre and post-infection scans.

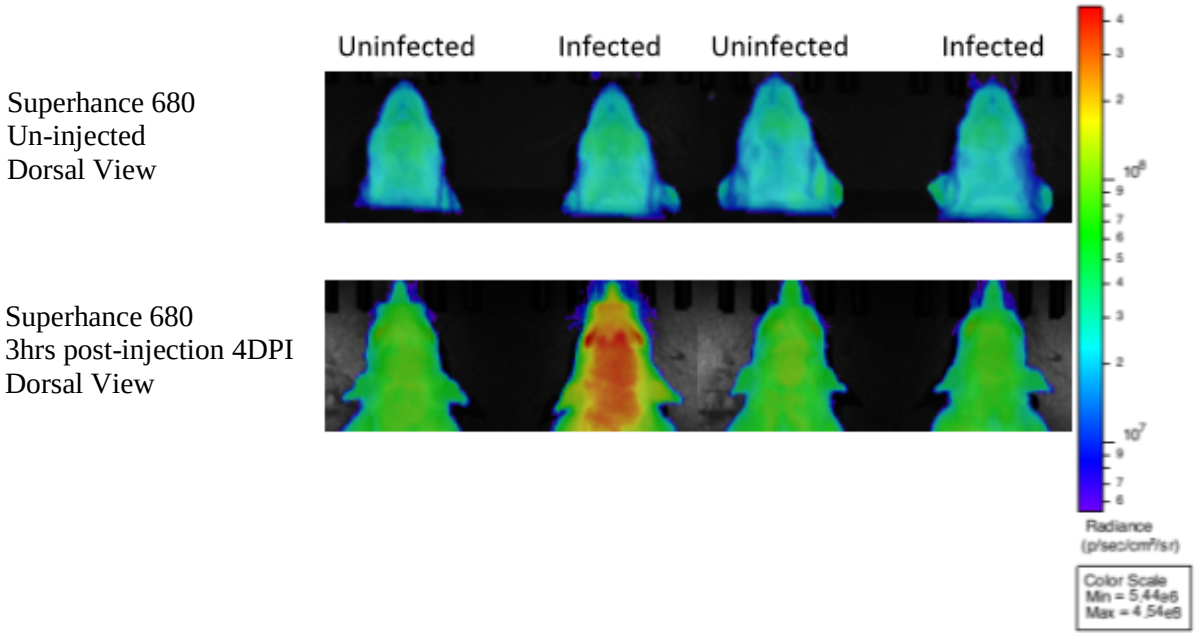

Figure 15. Early time point comparison using IVIS imaging

Superhance 680, a small fluorescent *in vivo* blood pool-imaging agent (MW = 1540) was injected into rats 4 days after RVFV aerosol infection. Rats were then imaged 3 hours later to observe vascular leakage in uninfected vs. infected rats. All imaging conditions were the same between pre and post-infection scans.

All IVIS imaging from un-injected Lewis rats showed no signs of breakdown of vascular integrity before Rift Valley fever virus infection. Based on the use of the fluorescent imaging agent Superhance 680 in conjunction with IVIS imaging (Figure 13), the total flux measured in RVFV infected rat brains was significantly different than the total flux measured in uninfected rat brains. The total flux was measured by detecting the quantity of Superhance present in the brain after vascular leakage. A significant difference in flux between infected and uninfected rats occurred on 6DPI ($p = 0.016$). Surprisingly, although there appears to be more fluorescence in the 6DPI extracted brains of infected rats compared to controls, the difference was not significant in terms of total flux. Natural autofluorescence due to skin and fur interactions while in the IVIS

chamber may have impacted the overall imaging results. When multiple angles of imaging were tested using Superhance 680 (Figure 14), similar differences were visualized relating to vascular breakdown between infected and uninfected rats comparable to Figure 13. Angles showing the ventral view, left lateral view, and right lateral view indicated that all infected rats at 5DPI experienced vascular breakdown while uninfected animals maintained vascular integrity. We next tested an early infection time point (4DPI) using Superhance 680 (Figure 15). We did this to see if breakdown of the CNS vasculature occurred before the clinical window (5-7DPI). The first pair of rats imaged three hours (4DPI) following the injection of Superhance 680 demonstrated breakdown of the vasculature in the infected rat, while the uninfected rat maintained vascular integrity. The second group of rats did not produce the same visual differences between the infected and uninfected rats as was clearly illustrated between the rats in the first set of images. Instead, both infected and uninfected rats in the second group appeared healthy based on the lack of vascular leakage. This was interesting because the same imaging conditions were replicated and both infected rats received the same aerosolized dose of RVFV.

Because Superhance 680 was not detected in the CNS tissues of Lewis rats before 4 - 5DPI, an assay utilizing a fluorescent agent with a smaller molecular weight was implemented to detect CNS vascular disruption at an earlier time point (Figure 16). We ran a fluorescein isothiocyanate (FITC – Sigma Aldrich MW = 376) assay on two separate cohorts of aerosol infected rats that were serially sacrificed (3/DPI). FITC salt was injected into the tail vein of each rat two minutes before euthanasia. Serum samples and brain samples were then collected and FITC salt content was extracted and read on a plate fluorometer. Comparing the concentration of FITC in the serum samples normalized FITC concentrations in brain samples. The levels of

FITC vascular leakage in the olfactory bulb, cortex, and cerebellum were then compared to respective viral load content measured by Q-RT-PCR in each of the tissues.

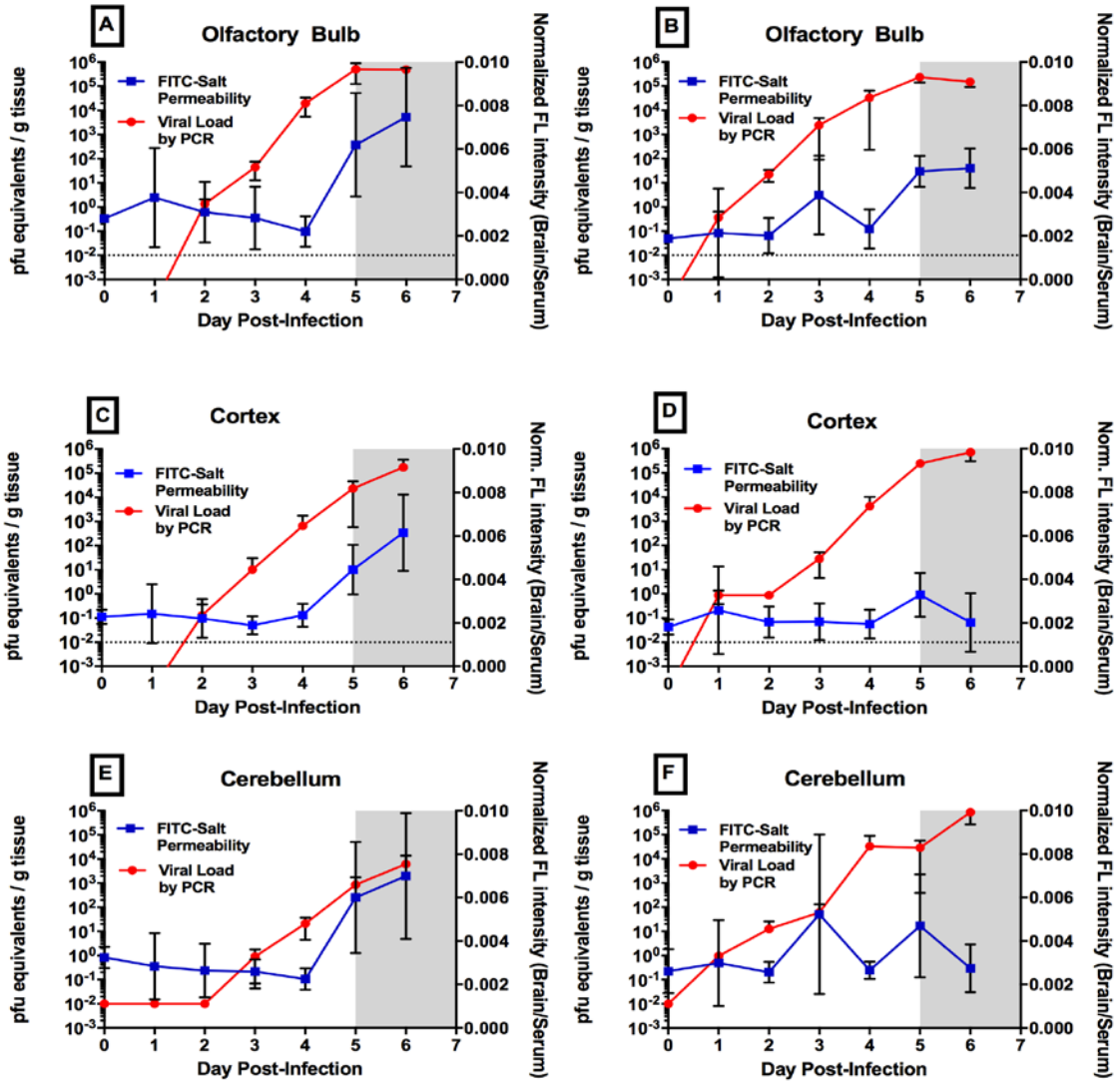

Figure 16. Vascular integrity determined by fluorescein isothiocyanate (FITC) salt assay

Fluorescein isothiocyanate (FITC) salt (MW = 376) was injected into rats two minutes prior to euthanasia each DPI to measure blood brain barrier breakdown and vascular leakage. The levels of FITC vascular leakage in the olfactory bulb, cortex, and cerebellum were compared to respective viral load content measured by Q-RT-PCR in each of the tissues. Each CNS tissue was replicated across two separate experiments. In (A), (C), and (E) rats were infected with RVFV via aerosol at a dose of 1.0 x 10^3 pfu/animal. In (B), (D), and (F) rats were infected with RVFV via aerosol at a dose of 2.0 x 10^4 pfu/animal.

Based on the fluorescein salt isolation from serially sacrificed Lewis rats (Figure 16), only very low levels of FITC salt could be detected due to CNS vascular leakage before the clinical window of infection (5DPI – 7DPI). This clinical window vascular leakage is especially evident in both experiments testing the olfactory bulb (A and B), the first experiment testing the cortex (C), and the first experiment testing the cerebellum (E). The second experiment testing the cortex (D) and cerebellum (F) indicate that vascular leakage is not occurring during the clinical window in these tissues. The PCR data plotted next to each FITC result shows a comparison between the amounts of virus in each CNS tissue versus how much vascular leakage is occurring.

5.0 DISCUSSION

Documentation from recent outbreaks of RVF (Kenya, East Africa, Sudan, and Tanzania from 2006-2008) has indicated that the epidemiology of RVFV is most likely changing (8). Analysis from historical outbreaks demonstrated that viral infection was most prominent in livestock populations (8). Data analysis from recent outbreaks suggests that more human cases are emerging than in previously documented RVFV outbreaks. Not only are more human cases emerging, but also the mortality rate from human infection is increasing when compared to mortality rates from historical RVFV outbreaks (6). A documented outbreak that occurred in South Africa in 2010 left at least 26 dead from the 237 total cases. These data support that an epidemiological change in the lethality of the virus is underway (6).

Recent scientific research has identified that aerosolization of RVFV is the most likely route of infection for a bioterrorism event. This is due to the high mortality rate caused by aerosolization of small viral particulates and the ease of dissemination in a heavily populated area (6). Aerosolization can also occur naturally during animal slaughter and butchering. Identifying the system of viral pathogenesis during various routes of infection studied in the current research is a crucial first step in the successful development of a vaccine or therapeutic that may prevent or limit RVFV progression from reaching the hemorrhagic or encephalitic forms.

Due to both the possibility of a bioterrorism event or the natural spread of RVFV (which appears to be developing higher infection and mortality rates among humans), it is important to possess a relevant animal model to successfully test various infection routes. The current research implemented the same Lewis rat model previously described in order to test the targeted infection routes, and to understand the pathogenesis of RVFV after viral administration. The rat model was also implemented in an attempt to quantify the distribution of virus and to identify the progression of viral migration *in vivo* throughout each DPI (1-7), specifically progression in CNS tissues.

The first step we took in assessing the clinical outcome in RVFV infected Lewis rats was to compare survival based on the different routes of infection: aerosol, subcutaneous, intranasal, intratracheal, and intragastric. The Hartman lab had previously established that aerosol infection of Lewis rats with RVFV caused lethal encephalitis (13). We wanted to determine whether depositing viral particles in the lungs only (intratracheal infection) or the nasal mucosa only (intranasal infection) would impact the outcome of respiratory tract RVFV infection. We chose to test the intragastric route of infection to determine if successful infection by RVFV of the gastrointestinal tract could be initiated. This route of infection may occur in a natural setting due to the consumption of infected meat. It is also possible that RVFV particles may be deposited in the gastrointestinal tract after aerosol exposure. We chose to test the subcutaneous route of infection because it represents a natural route of infection. It has also been historically shown that Lewis rats are resistant to subcutaneous infection with RVFV (13). We expected that the subcutaneous route of infection would serve as the negative control.

Aerosol and intranasal infection mirrored one another in that 100% mortality was caused and neurological disease progression and encephalitis onset was very rapid. Weight and

temperature data acquired from both cohorts also showed that all rats involved displayed elevated temperatures, and many displayed significant weight loss before euthanasia due to the onset of neurological symptoms. PCR data acquired from aerosol infection, regardless of dose, indicated that a strong viral presence was detected in the CNS tissues during the clinical window of infection (5-7DPI), which would explain the onset of neurological symptoms occurring in these animals. Together, these data from both aerosol and intranasal routes of infection agree with our hypothesis that viral deposition in the respiratory tract, specifically the nasal mucosa, leads to encephalitis and death.

Subcutaneous and intragastric infection routes displayed the lowest mortality rates and the progression of disease onset was also variable with euthanasia due to neurological symptoms ranging from 6DPI up to 18DPI. We expected the intragastric route of infection to cause a very low mortality rate due to the composition of the gastrointestinal tract and its ability to breakdown and digest foreign particles, but the results did not reflect this expectation. We believe it is possible that successful infection of RVFV was initiated at the site of the vagus nerve, which would explain how the virus then reached the brain and initiated replication. Temperature data (intragastric only) and neurological symptoms were clear indicators for viral infection while weight loss remained variable between both infection routes. PCR data from both subcutaneous and intragastric infection routes (only endpoint data for intragastric infection) indicate viral presence was maintained in peripheral tissues throughout the course of both experiments. The main difference between intragastric infection and subcutaneous infection routes was the mortality rate. We were surprised to see an almost 50% mortality rate from the intragastric route of infection while we expected to see almost no mortality from the subcutaneous route of infection. Another difference between intragastric and subcutaneous infection routes occurred in

the PCR analysis of CNS tissues. Intragastric infected rats displayed high viral titers in CNS tissues at endpoint, while subcutaneous infected rats maintained a very low viral titer in CNS tissues. This difference may be due to having acquired tissues longitudinally from subcutaneous infected rats while only endpoint tissues were collected from intragastric infected rats. Based on the previous data, both subcutaneous and intragastric infection routes were vastly different than the previously established aerosol model of Lewis rat infection. Virus was still detected in the CNS tissues of both intragastric and subcutaneous infected rats, which explains how the onset of neurological disease and encephalitis lead to euthanasia. The low mortality rate from subcutaneous infected rats supports our hypothesis that severe disease development was lower compared to infection routes that deposit virus in the respiratory tract. The mortality rate of the intragastric infected cohort opposed our hypothesis. We did not expect to see such a high mortality rate, which may indicate that RVFV is able to initiate successful infection in the gastrointestinal tract. An alternate explanation may be that virus was aspirated into the respiratory tract after intragastric inoculation, which could have caused infection similar to intratracheal inoculation. Because PCR detection showed viral RNA in the CNS tissues of subcutaneous infected rats, a future experiment testing if infectious virus actually replicates in the CNS tissues of subcutaneous infected animals would be useful in determining if viral penetration into the CNS is critical to establishing severe clinical outcome.

The intratracheal infected cohort displayed a high mortality rate after infection with RVFV. We expected a high mortality rate because of the viral deposition in the respiratory tract. Because 100% mortality was not achieved, this may indicate that viral deposition in the nasal mucosa (as seen with intranasal infection) is more important in establishing severe neurological disease and encephalitis than viral deposition in the lungs alone. These data also suggested that

fever onset and neurological symptoms were indicators for severe disease onset. Weight change was variable and therefore not a reliable identifier of infection. Taken together, these data indicate that intranasal infection leads to disease onset and generates a mortality rate most comparable to aerosol infection, which suggests that viral deposition in the upper respiratory tract is more likely to cause fatal disease.

Because of the vast differences noted between aerosol infection and subcutaneous infection, we wanted to explore how cellular function was impacted *in vivo* based on these viral routes. We know that subcutaneous infection causes low mortality and that when infection does occur the timing of disease onset is delayed. We also know that aerosol infection causes 100% mortality and displays rapid onset of neurological disease. To explore the differences between subcutaneous and aerosol infection routes, we used the Abaxis Vetscan HM2 Hematology Blood Analyzer (HM2) to measure complete blood counts (CBC). This enabled us to acquire cellular information specifically relating to white blood cells, platelets, and red blood cells. Serial sacrifice blood analysis of aerosol infected, subcutaneous, and control rats occurred on 3DPI – 7DPI. Lymphocyte counts and platelet counts in aerosol infected animals were significantly lower than control counts throughout the course of the experiment. This indication of lymphocytopenia and thrombocytopenia in aerosol infection agrees with previously described data acquired by the Hartman lab and fits with the Lewis rat model. Lymphocyte counts and platelet counts in subcutaneous infected animals showed variation, but no values were significantly different than control counts. Granulocyte counts in aerosol infected animals were significantly higher than control granulocyte counts. This indication of granulocytosis in aerosol infection agrees with previously described data acquired by the Hartman lab and fits with the Lewis rat model. Granulocyte levels in subcutaneous infected animals were not significantly

different than control values. Based on these data, aerosol infected rats exhibited lymphocytopenia, granulocytosis, and thrombocytopenia, which agreed with the previously established aerosol Lewis rat model. Subcutaneous infected animals lack these characteristic alterations in blood cell counts. These findings help explain why such a vast difference in mortality and severe clinical outcome was recorded between subcutaneous and aerosol infected rats.

We next focused on measuring the vascular integrity of the brain in RVFV aerosol infected Lewis rats to determine if breakdown of the blood brain barrier occurs. We first attempted to visualize the occurrence of vascular leakage by incorporating the Spectrum CT In Vivo Imaging System (IVIS). This allowed us to use fluorescent imaging technology in combination with a fluorescent imaging agent (Superhance 680) to visualize vascular leakage. The first group of rats we imaged on 4DPI in order to target a time point prior to the clinical window (5-7DPI). We reasoned that perhaps on 4DPI the initiation of the blood brain barrier breakdown would begin. After analysis of the images, the first group of rats we imaged showed a significant difference in vascular breakdown between infected and uninfected rats. The second group of rats we imaged showed no difference in vascular breakdown between infected and uninfected rats. Because IVIS imaging technology in conjunction with RVFV exploration is not common practice in the scientific community, determining what fluorescent agent was most effective at a specific time point was very difficult. Also, even though Lewis rats are inbred, we have found that disease progresses at different rates within each cohort. We reasoned that perhaps the visual difference between the two sets of rats occurred because the second infected rat had not yet experienced breakdown of CNS vasculature. We left the rats from the first imaging session overnight and attempted imaging on 5DPI (onset of clinical window).

Interestingly enough we saw a complete change in the infected rat that on the previous day (4DPI) showed no significant vascular leakage differences from the control rat. On 5DPI there was a significant difference in vascular leakage between the infected and uninfected rat in the second rat group. The first group also maintained a significant difference in vascular leakage between the infected and uninfected rat on 5DPI. This vascular breakdown on 5DPI in both groups of rats agrees with the previously established clinical window of infection (5-7DPI) in the Lewis rat model. We then left the rats in their cages overnight and imaged both pairs one final time on 6DPI. Initially we expected the agent to be completely cleared from the system because Superhance 680 is recommended for use between 0.5 – 24hrs post-injection. To our surprise, both groups of rats still displayed significant differences in vascular leakage between infected and uninfected animals on 6DPI. We then extracted the brain from each rat for *ex vivo* imaging to ensure that there was no significant background fluorescence. Though the vascular breakdown comparison between infected and uninfected rat brains was not significantly different, there was clear indication that vascular breakdown was more evident in infected rats. Based on this imaging data, we know that 4 - 5DPI is when visible CNS vascular leakage begins through the use of the IVIS and Superhance 680. This supports our hypothesis that vascular leakage occurs in the brain during the onset of clinical symptoms.

We know that virus is present in CNS tissues in aerosol infected rats earlier than 4DPI from previously described PCR data. We wanted to test a smaller molecular weight molecule (Fluorescein Isothiocyanate – MW 376) other than Superhance 680 (MW 1540). We reasoned that a smaller molecular weight molecule way be able to penetrate smaller breaks in vasculature that occur at an earlier time point. To test this theory, we ran a FITC salt assay on two separate cohorts of aerosol infected rats that were serially sacrificed (3/DPI). Analysis showed that only

low levels of FITC salt could be detected before the clinical window of infection (5-7DPI) was reached. During the clinical window, FITC salt levels rose indicating that more significant breakdown of the vasculature in the CNS was occurring. The aerosol PCR data discussed previously was then transposed next to the FITC data for each tissue of interest. Important to note from this transposition is that viral load in brain tissues increases approximately two days earlier than FITC salt detection increases. This indicates that the virus enters the CNS using a route other than hematogenous spread from the blood to the brain. These results not only agree with the previously discussed IVIS data, but also support our hypothesis that vascular leakage occurs in the brain during the onset of clinical symptoms (5-7DPI).

Taken together, these data indicate that the nasal epithelium appears to be a critical site for deposition of RVFV in order to establish severe encephalitis in rats. We know this due to the infection route survival curve and weight/temperature data that indicates nasal epithelium deposition leads to most rapid disease onset and 100% mortality due to lethal encephalitis. We also know that disruption of the blood brain barrier begins 4 - 5DPI. We know this to be accurate from both the IVIS imaging data and the FITC salt assay, in which both sets of data complement one another. We also know from the PCR data that vascular leakage is not necessary for entrance of the virus into the CNS tissues due to the fact that virus is present in the brain two days before leakage can be detected.

We now know that RVFV infection routes that deposit virus in the respiratory tract, more specifically the nasal mucosa, are more likely to generate higher mortality due to neurological disease. This information may be critical for the proper development of either a therapeutic or vaccine for future use. We also know that virus is not initially reaching the brain through hematogenous spread from the vascular breakdown of the blood brain barrier. Future therapeutic

and vaccine development attempts can instead target a different route of viral entry such as spread to the brain via the olfactory nerves. Overall, there is still a need for more in-depth understanding of the neuropathological mechanisms involved in propagating RVFV throughout the host until eventual deposit in the CNS.

BIBLIOGRAPHY

1. Nanyingi, M., et al., "A systematic review of Rift Valley Fever epidemiology 1931-2014." *Infection Ecology & Epidemiology,* 5 (2015). Web.

2. Pal, M., et al., "Rift Valley Fever: A Fatal Viral Disease of Neonatal Animals." *International Journal of Livestock Research,* 2.2 (2012): 14-20. Web.

3. Nakouné, E., et al., "Rift Valley Fever Virus Circulating among Ruminants, Mosquitoes and Humans in the Central African Republic." *PLoS Neglected Tropical Diseases,* 10 (2016). Web.

4. Balenghien, T., et al., "Towards a better understanding of Rift Valley fever epidemiology in the south-west of the Indian Ocean." *Veterinary Research*, 44 (2013). Web.

5. Balkhy, HH., Memish, ZA., "Rift Valley fever: an uninvited zoonosis in the Arabian Peninsula." *International journal of antimicrobial agents*, 21 (2003). Web.

6. Mandell, R., "Rift Valley Fever Virus: A Real Bioterror Threat." *Journal of Bioterrorism & Biodefense,* 2 (2011). Web.

7. Wichgers Schreur, PJ., et al., "Four-segmented Rift Valley fever virus induces sterile immunity in sheep after a single vaccination." *Vaccine,* 33 (2015). Web.

8. Himeidan, YE., et al., "Recent Outbreaks of Rift Valley Fever in East Africa and the Middle East." *Frontiers in Public Health,* 2 (2014), Web.

9. "Rift Valley Fever." *World Health Organization*. World Health Organization. 2016. Web. Available from: http://www.who.int/mediacentre/factsheets/fs207/en/

10. Scharton, D., et al., "Favipiravir (T-705) protects against peracute Rift Valley fever virus infection and reduces delayed-onset neurologic disease observed with ribavirin treatment." *Antiviral Research,* 104 (2014), Web.

11. "Rift Valley Fever." *Centers for Disease Control and Prevention.* Centers for Disease Control and Prevention. 2013. Web. Available from: https://www.cdc.gov/vhf/rvf/

12. Bouloy, M., Flick, R., “Reverse genetics technology for Rift Valley fever virus: Current and future application for the development of therapeutics and vaccines.” *Antiviral Research,* 84 (2009), Web.

13. Bales, J., et al., “Choice of inbred rat strain impacts lethality and disease course after respiratory infection with Rift Valley Fever Virus.” *Frontiers in Cellular and Infection Microbiology,* 2 (2012), Web.

14. Peters, CJ., Slone, TW., “Inbred rat strains mimic the disparate human response to Rift Valley fever virus infection.” *Journal of Medical Virology,* 10 (1982), Web.

15. Caroline, A., et al., “Inflammatory Biomarkers Associated with Lethat Rift Valley Fever Encephalitis in the Lewis Rat Model.” *Frontiers in Microbiology,* 6 (2015), Web.

16. Reed, D.S., et al., “Differences in aerosolization of Rift Valley Fever virus resulting from choice of inhalation exposure chamber: implications for animal challenge studies.” *Pathogens and Disease,* 71 (2014), Web.

17. Caroline, A., et al., “Broad Spectrum Antiviral Activity of Favipiravir (T-705): Protection from Highly Lethal Inhalational Rift Valley Fever.” *Plos Neglected Tropical Diseases,* 8 (2014), Web.